Am J Physiol Renal Physiol 291: F1224–F1231, 2006.
First published May 30, 2006; doi:10.1152/ajprenal.00307.2005.

Functional roles of cationic amino acid residues in the sodium-dicarboxylate cotransporter 3 (NaDC-3) from winter flounder

Yohannes Hagos, Jürgen Steffgen, Ahsan N. Rizwan, Denis Langheit, Ariane Knoll, Gerhard Burckhardt, and Birgitta C. Burckhardt

Zentrum Physiologie und Pathophysiologie, Abteilung Vegetative Physiologie und Pathophysiologie, Göttingen, Germany

Submitted 29 July 2005; accepted in final form 18 May 2006

Hagos, Yohannes, Jürgen Steffgen, Ahsan N. Rizwan, Denis Langheit, Ariane Knoll, Gerhard Burckhardt, and Birgitta C. Burckhardt. Functional roles of cationic amino acid residues in the sodium-dicarboxylate cotransporter 3 (NaDC-3) from winter flounder. *Am J Physiol Renal Physiol* 291: F1224–F1231, 2006. First published May 30, 2006; doi:10.1152/ajprenal.00307.2005.—In the present study, we determined the functional role of 15 positively charged amino acid residues at or within 1 of the predicted 11 transmembrane helixes of the flounder renal sodium-dicarboxylate cotransporter fNaDC-3. Using site-directed mutagenesis, histidine (H), lysine (K), and arginine (R) residues of fNaDC-3 were replaced by alanine (A), isoleucine (I), or leucine (L). Most mutants showed sodium-dependent, lithium-inhibitable [^{14}C]succinate uptake and, in two-electrode voltage-clamp (TEVC) experiments, K_m and ΔI_{max} values comparable to wild-type (WT) fNaDC-3. The replacement of R109 and R110 by alanine and isoleucine (RR109/110AI) prevented the expression of fNaDC-3 at the plasma membrane. When the lysines at positions 232 and 235 were replaced by isoleucine (KK232/235II), the transporter was expressed but showed small transport rates and succinate-induced currents. K114I, located within transmembrane helix 4, showed [^{14}C]succinate uptake similar to WT but relatively small inward currents. When K114 was replaced by arginine, glutamic acid (E), or glutamine (Q), all mutants were expressed at the cell surface. In [^{14}C]succinate uptake and TEVC experiments performed simultaneously on the same oocytes, uptake was similar to or higher than WT, whereas succinate-induced currents were either comparable (K114R) to, or considerably smaller (K114E, K114I, K114Q) than, those evoked by WT. These results suggest that a positively charged residue at position 114 is required for electrogenic sodium-dicarboxylate cotransport.

sodium/dicarboxylate cotransport; electrogenicity; SLC13A3; mutational analysis; basic amino acids

SODIUM-DEPENDENT DICARBOXYLATE transporter type 3 (NaDC-3), present in the brain (10), eye, optic nerve (6), liver (4), and kidneys (4, 20, 30), serves important physiological functions. In astrocytes, NaDC-3 plays a role in the process of myelination by taking up *N*-acetyl-aspartate into the cells (10). Recent studies described the presence of NaDC-3 in the optic nerve and retina and discussed the possible involvement of the transporter in Canavan disease, a genetic disorder associated with optic neuropathy (6). In the liver, NaDC-3 is located at the sinusoidal membrane of perivenous hepatocytes. These cells are involved in scavenging the toxic ammonia from the blood by utilizing it for glutamine synthesis. NaDC-3 provides perivenous hepatocytes with α-ketoglutarate needed for glutamine synthesis (4).

In renal proximal tubules, NaDC-3 is located at the basolateral cell membrane (9, 33) and serves two functions. First, NaDC-3 maintains an outwardly directed gradient of α-ketoglutarate driving the organic anion/dicarboxylate exchangers OAT1 (29, 35) and OAT3 (1, 31) and, thus, secretion of a large number of organic anions including widely used drugs and environmental toxins (2). Second, NaDC-3 as well as NaDC-1 provide proximal tubule cells with di- and tricarboxylates required for energy metabolism and gluconeogenesis (34). Studies in human and rat kidneys of different ages have demonstrated a higher abundance of NaDC-3 protein in older subjects (33). Although this may be beneficial for the supply of energy, the production of oxygen radicals is also increased, which may lead to damage of proximal tubule cells. In this respect, it is interesting that NaDC-3 exhibits a significant homology with INDY, the sodium-independent dicarboxylate transporter of *Drosophila melanogaster* (11, 14). A functional defect of INDY by mutation resulted in life span extension of the fly (27).

NaDC-3s have been cloned from a variety of species, including humans, the rat, mouse, flounder, and *Xenopus laevis* (4, 16, 20, 30, 32). They are members of the SLC13 gene family of the sodium-coupled anion transporters (15), and their gene is termed SLC13A3. This gene family includes also the NaDC-1s, sodium-dependent dicarboxylate transporters located at the luminal membrane of proximal tubule cells (15, 19). In most species, NaDC-1 shows a lower affinity for succinate than does NaDC-3 (17). In addition, the sodium-coupled citrate transporter NaCT (SLC13A5), which has a higher affinity for citrate than for succinate, also belongs to this gene family (12, 19). The predicted secondary structure of all SLC13 members revealed 11 transmembrane (TM) domains with an intracellular NH_2 terminus and an extracellular COOH terminus (18, 37). On functional expression in *X. laevis* oocytes (21, 30) or cell lines (13, 24), NaDC-1s as well as NaDC-3s from different species showed sodium-dependent substrate uptake or substrate-associated inward currents (21, 30), indicating an electrogenic cotransport of three sodium ions with one divalent succinate. This stoichiometry was proven by simultaneous measurements of succinate uptake and succinate-induced current in the same oocyte (5, 13, 28).

The aim of the present study was to explore the potential functional role of positively charged amino acid residues at or within one of the putative TM domains of NaDC-3 from winter flounder kidney. Basic amino acids at the borders of TM helixes may be involved in proper positioning of these seg-

Address for reprint requests and other correspondence: Y. Hagos, Zentrum Physiologie und Pathophysiologie, Abt. Vegetative Physiologie und Pathophysiologie Universität Göttingen, Humboldtallee 23, 37073 Göttingen, Germany (e-mail: hagos@physiol.med.uni-goettingen.de).

The costs of publication of this article were defrayed in part by the payment of page charges. The article must therefore be hereby marked "*advertisement*" in accordance with 18 U.S.C. Section 1734 solely to indicate this fact.

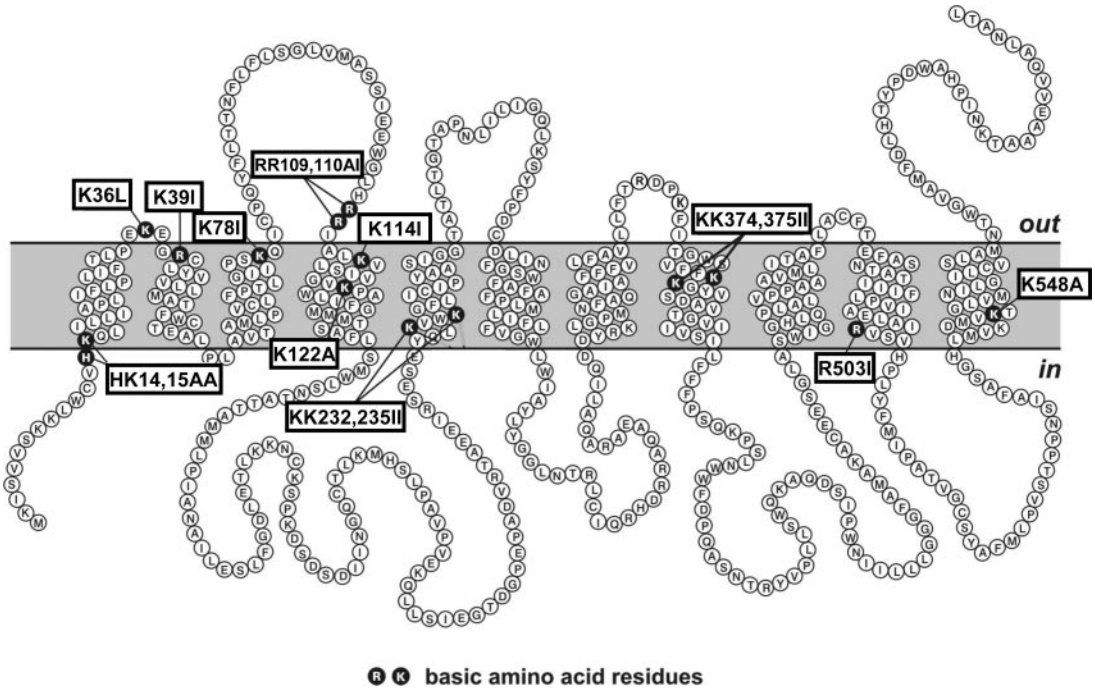

Fig. 1. Model of putative secondary structure of flounder renal sodium-dicarboxylate cotransporter (fNaDC-3). Prediction of the secondary structure of fNaDC-3 was performed with TopPred 2 (http://bioweb.pasteur.fr/seqanal/interfaces/toppred.html). Amino acids are indicated by single letter code. Each of the highlighted amino acids was mutated by site-directed mutagenesis.

ments within the lipid bilayer, and those within TM helixes may form salt bridges and/or interact with charged substrates. By site-directed mutagenesis, we replaced 15 positively charged amino acids [arginine (R), histidine (H), and lysine (K); for location, see Fig. 1] and functionally characterized the mutants by measuring [^{14}C]succinate uptake and succinate-induced inward currents.

MATERIALS AND METHODS

Expression of NaDC-3 and mutants. Stage V and VI oocytes from *X. laevis* (Nasco, Ft. Atkinson, WI) were prepared by overnight treatment in control solution (in mM: 110 NaCl, 3 KCl, 2 $CaCl_2$, 5 HEPES/Tris, pH 7.5) supplemented with collagenase (type CLSII, Biochrom, Berlin, Germany). Subsequently, after being washed with Ca^{2+}-free control solution to remove adhering follicle cells, the oocytes were injected with 23 nl of 1 μg/μl cRNA prepared either from the wild-type (WT) clone, from one of the mutants, or an equivalent volume of H_2O ("mock" oocytes). Afterward, injected oocytes were incubated for 3 days at 16–18°C in control solution supplemented with gentamicin (12 mg/ml) and 2.5 mM sodium pyruvate. The medium was changed daily, and damaged oocytes were discarded.

In vitro cRNA synthesis. The cDNA of WT winter flounder NaDC-3 (fNaDC-3) and of the mutants was used for in vitro cRNA synthesis. Initially, plasmids of WT and mutants were linearized with *Not*I restriction. In vitro transcription was carried out using a T7 mMessage mMachine kit (Ambion, Austin, TX). After purification the cRNA by phenol-chloroform extraction, the cRNA was resuspended in water and adjusted to a final concentration of 1 μg/μl.

Site-directed mutagenesis. The basic amino acids (arginine, histidine, and lysine) located within or close to the putative TM domains of fNaDC-3 were mutated to neutral amino acids [alanine (A), isoleucine (I), or leucine (L)]. We generated single mutants or, in the case of two adjacent positively charged amino acid residues, double mutants. The lysine at position 114 was replaced by isoleucine and, additionally, by glutamine (Q), glutamate (E), or arginine (R). All mutations were performed by using a QuikChange site-directed mutagenesis kit (Stratagene, Cambridge, UK). To verify the success of site-directed mutagenesis, both strands of the mutants were sequenced by dye- terminated cycle sequencing using specific fNaDC-3 primers. After purification, the PCR products were sequenced using an ABI automatic sequencer (ABI 377, Applied Biosystems, Weiterstadt, Germany). Table 1 includes the primers used for inserting the mutation in the WT NaDC-3 cDNA sequence.

Electrophysiological studies. These studies were carried out 3 days after cRNA injection at room temperature. Current recordings were made using the two-electrode voltage-clamp technique (TEVC) with a commercial amplifier (OC725, Warner, Hamden, CT). Microelectrodes were filled with 3 M KCl and had resistances of ~1 MΩ. The resting membrane potential of the oocytes ranged between −28 and −46 mV, and holding currents to achieve a potential of −60 mV were in the range of −10 to −40 nA. Steady-state currents were obtained during 5-s voltage pulses from −60 mV to potentials between −90 and 0 mV in 10-mV steps. The current-voltage (*I-V*) relationships for

Table 1. *Primers used for site-directed mutagenesis*

Mutant	Sense Primer Sequence
HK14/15AA	GCTGTGGTGCGTCGCCGCGCAGCTGATCCTGC
K36L	CTCTGCCCGAACTGGAGGGAAGATGTCTTTACG
R39I	GCCCGAAAAGGAGGGAATATGTCTTTACGTGG
K78I	GGAATCATTCCGTCGATACAGATCTGCCCTCAG
RR109/110AI	GGAGTGGGGCCTGCATGCCATAATCGCTCTGAAG
K114I	CGCAGAATCGCTCTGATTGTCCTGAGCATCGTG
K122A	GCATCGTGGGAGTGGCCCCAGCCTGGCTC
KK232/235II	CGGAGTATCAGCTGATTGTGTGGATAGGATTC-CTGATCTGTATTC
KK374/375II	CCGGCTGGTCTGTGTTCTTTATAATAGGGTATGTCTC
R503I	CTGAACTGGCCATTATTGTGTCAGTGCACCC
K548A	GGTCAAAGACATGGTGGCGACTGGCTTCGTAATG

Bold and underlined nucleotides reflect the position of the mutation.

substrate-induced currents, ΔI, were determined by subtraction of the steady-state currents in the absence of the substrate from currents in the presence of the substrate, respectively. For kinetic experiments, oocytes were superfused with buffers of succinate concentrations up to 10 mM, and the induced currents were recorded at −60 mV. The kinetic parameters, K_m and ΔI_{max}, were obtained by Eadie-Hofstee analysis.

Succinate uptake experiments. Expression of WT NaDC-3 and mutants in oocytes was confirmed by comparing the uptake of radiolabeled succinate between cRNA- and water-injected mock oocytes. Uptake of [^{14}C]succinate (15–60 mCi/mmol; NEN Life Science Products, Cologne, Germany) in oocytes was assayed for 30 min at room temperature in control solution containing in addition 18 μM labeled succinate. The sodium-free buffer was obtained by replacing NaCl by tetramethylammonium chloride (TMACl). In this case, the pH was adjusted to 7.4 by 1 M TMAOH. [^{14}C]Succinate uptake was stopped by aspiration of the incubation medium and several washes of the oocytes in ice-cold control solution. Oocytes were lysed in 1 M NaOH, and liquid scintillation counting was performed as described elsewhere (8). In a second set of experiments, uptake of [^{14}C]succinate was measured under voltage-clamp conditions in oocytes expressing WT and mutant transporters. Oocytes were clamped at −60 mV, and 18 μM [^{14}C]succinate plus 50 μM unlabeled succinate was applied for 30 min directly in the bath at stopped perfusion. Afterward, the perfusion was restarted and the substrate was washed out. To remove any nonspecific radioactivity transferred by the pipette, the oocyte was washed briefly in four petri dishes filled with ice-cold control solution before transferal to scintillation vials, where oocytes were lysed in 1 M NaOH, and liquid scintillation counting was performed as described (8).

Immunohistochemistry of NaDC-3 surface expression. Surface staining of WT and mutants was performed with a specific antibody generated in rabbits using a fNaDC-3-specific antigen (CKSP-KDSDSDII; Eurogentec, Seraing, Belgium). Manually devitellinized oocytes were incubated for 5–10 min in 200 mM potassium aspartate, followed by an overnight fixation at −20°C in Dent's solution (80% methanol/20% DMSO). After removal of the fixation solution, oocytes were incubated overnight at −4°C in 10% goat serum containing the anti-fNaDC-3 antibody in a dilution at 1:50. Afterward, the primary antibody was washed out with PBS (in mM: 140 NaCl, 4 KCl, 2 K_2HPO_4), and the oocytes were incubated with the secondary antibody (Alexa Fluor 488 goat anti-rabbit) at a dilution of 1:200 (Molecular Probes, Eugene, OR) for 1 h. To remove nonspecific labeling of the secondary antibody, the oocytes were washed several times with PBS and fixed for 30 min with 3.7% paraformaldehyde. The oocytes were embedded in acrylamide (Technovit 7100, Kulzer, South Bend, IN) according to the manufacturer's instructions. Five-micrometer sections from the embedded oocytes were analyzed with a fluorescence microscope (Zeiss Axiovert S100TV, Jena, Germany) supported by digital imaging (Metamorph software, Universal Imaging, Jena, Germany).

Chemicals. Unless otherwise specified, all chemicals were of analytic grade and purchased from Sigma (Taufkirchen, Germany) or Merck (Darmstadt, Germany).

Data analysis. Data are expressed as means ± SE. All experiments were repeated with oocytes from at least two different frogs. Student's *t*-test was used to reveal statistical significance at $P < 0.01$.

RESULTS

Function of WT and mutant fNaDC3. To investigate whether positively charged amino acids located in or near putative TM domains are important for function, we generated the mutants shown in Fig. 1. Initially, we tried to generate alanine mutants, but for unknown reasons some mutations containing the DNA codon for alanine did not form colonies after transformation of the mutant plasmid into *Escherichia coli* and incubation overnight. Therefore, we replaced the codons for other neutral amino acids such as isoleucine, resulting in successful growth of the colonies.

Table 2. *[^{14}C]succinate uptake of wild-type fNaDC-3 and mutants*

Mutant	110 mM NaCl	110 mM TMACl	10 mM LiCl plus 100 mM NaCl	110 mM LiCl
fNaDC-3 (WT)	100.0±5.5	5.6±1.2	43.3±6.3	23.1±1.6
HK14/15AA	95.7±19.3	10.0±3.0	36.6±3.0	2.9±0.3
K36L	73.1±4.7	0.7±0.1	38.3±2.9	15.0±1.8
R39I	114.0±7.7	ND	ND	ND
K78I	103.9±10.9	ND	ND	ND
RR109/110AI	5.6±1.4*	1.53±0.4	ND	ND
K114I	138±16.7*	7.5±2.1	52.2±12.0	10.9±3.6
K122A	130±10.7	0.4±0.1	41.0±3.9	21.6±1.5
KK232/235II	28.2±4.0*	ND	ND	ND
KK374/375II	66.8±5.7*	0.6±0.1	29.1±1.6	7.7±0.4
R503I	124.7±10.4	ND	ND	ND
K548A	97.6±6.3	0.9±0.1	69.9±2.4	10.4±0.7

Values are means ± SE of 6–8 oocytes from 3–4 donors. All experiments were standardized by setting the wild-type (WT) [^{14}C]succinate uptake at each day to 100%. Uptake of 18 μM [^{14}C]succinate was determined for 30 min in oocytes expressing WT or mutants indicated in the first column. In 40 independent experiments using oocytes injected with an equal amount of cRNA, succinate uptake in WT was 275.0 ± 36.8 pmol·30 min^{-1}·oocyte^{-1}, and mock oocytes showed a nonspecific succinate uptake of 6.2 ± 0.9 pmol·30 min^{-1} ·oocyte^{-1}. Uptake buffer contained either 110 mM NaCl, 110 mM tetraethylammonium chloride (TMACl), 10 mM LiCl plus 100 mM NaCl, or 110 mM LiCl, respectively. ND, not determined. *$P < 0.01$ vs. WT fNaDC-3.

As shown in Table 2, most mutants were functional, i.e., they showed [^{14}C]succinate uptake in the presence of 110 mM NaCl. Thereby, succinate uptake for the mutants HK14/15AA, K36L, R39I, K78I, K122A, R503I, and K548A was not significantly different from that observed for WT. The mutants RR109/110AI, KK232/235II, and KK374/375II revealed significantly lower [^{14}C]succinate uptake, whereas K114I revealed significantly higher [^{14}C]succinate uptake rates compared with WT ($P < 0.01$). When NaCl was completely replaced by TMACl, succinate uptake by WT and the investigated mutants dropped to 10% or less of the uptake in the presence of sodium (Table 2, 110 mM TMACl). Hence, all tested mutants retained their sodium dependence. Where tested, 10 mM LiCl in the presence of sodium inhibited succinate uptake by WT and mutant fNaDC3 (Table 2, 10 mM LiCl, 100 mM NaCl), and some residual uptake of succinate was observed in the presence of 110 mM LiCl (Table 2, 110 mM LiCl), suggesting unaltered interaction with lithium of the tested mutants.

WT fNaDC-3 cotransports three Na^+ with one divalent succinate and, hence, generates an inward current, ΔI, in voltage-clamped oocytes (3). Here, we used the TEVC method to determine the kinetic parameters, K_m and ΔI_{max}, of WT fNaDC-3 and its mutants. In each experiment, various succinate concentrations ([S]) were used, and the data were analyzed according to Eadie-Hofstee (linear plots of ΔI against ΔI/[S]). For each mutant, the experiments were performed at least three times with oocytes from different donors. As summarized in Table 3, WT fNaDC-3 showed a mean K_m of 22 μM and an ΔI_{max} of −55 nA; the minus sign denotes an inward current. Most mutants showed an unchanged K_m. Mutant RR109/110AI did not show any detectable current, and with

Table 3. *Kinetic parameters determined by the 2-electrode voltage-clamp technique*

Mutant	K_m, μM	ΔI_{max}, nA	*n/m*
fNaDC-3 (WT)	21.6±10.6	−55±37	20/17
HK14/15AA	21.3±8.1	−66±18	7/4
K36L	8.9±5.3	−40±20	3/3
R39I	27.8±13.2	−121±25	6/4
K78I	36.0±5.9	−95±51	4/3
K114I		−12±9*	9/4
K122A	23.3±4.9	−41±10	6/4
KK232/235II		−7±4*	3/3
KK374/375II	6.0±4.7	−68±40	3/3
R503I	19.6±6.9	−67±1	4/3
K548A	27.0±15.2	−104±47	5/3

Values are means ± SE. *n,* No. of oocytes; *m*, number of donors. Succinate-induced currents were measured at various succinate concentrations at −60 mV. K_m and ΔI_{max} values were determined from Eadie-Hofstee plots. For the mutants K114I and KK232/235II, a saturation of the induced currents was not observed up to 10 mM succinate. In these 2 cases, ΔI_{max} is the current at 10 mM succinate. RR109/110AI is not included, because it did not show succinate-induced currents. *$P < 0.01$ vs. WT fNaDC-3.

mutants K114I and KK232/235II it was not possible to determine K_m and ΔI_{max} due to very low succinate-induced currents (Table 3). Among the mutants, we chose the substitutions at RR109/110, KK232/235, and K114 for further characterization.

Mutants RR109/110AI and KK232/235II. To determine whether the loss in transport activities (cf. Table 2) was due to defects in expression, immunohistochemical investigations were performed using polyclonal rabbit antibodies raised against a fNaDC-3-specific peptide. Whereas water-injected oocytes were negative due to the absence of endogenous NaDC-3 protein, WT-expressing oocytes showed a staining of the transporter protein at the surface of the oocyte (Fig. 2). In contrast, mutant RR109/110AI protein did not appear at the plasma membrane (Fig. 2, *bottom left*), which explains the very low [^{14}C]succinate uptake. As shown in Fig. 2 (*bottom right*), mutant KK232/235II protein did appear at the surface of the oocytes as visualized by staining, suggesting that the mutant is properly expressed but functionally defective.

Substitution of K114. The replacement of the positively charged lysine by uncharged isoleucine (K114I) resulted in a functional mutant (Table 2). However, in current-clamped oocytes, addition of succinate induced a relatively small depolarization (Fig. 3*A*). In WT-expressing oocytes, 1 mM succinate depolarized the membrane potential from −41.1 ± 3.1 to +6.4 ± 8.9 mV, i.e., by 47.5 mV. In K114I-expressing oocytes, the resting potential was comparable to that of WT (−41.6 ± 6.9 mV), but 1 mM succinate depolarized the oocytes by only 21.9 mV to −19.6 ± 4.6 mV. Next, we determined the *I-V* relationship of the succinate-induced currents. As shown in Fig. 3*B*, there is an almost linear relationship between the succinate-induced inward current and the clamp voltage in oocytes expressing WT fNaDC-3 (Fig. 3*B*, ●). Oocytes expressing mutant K114I again showed near-linear *I-V* relationships between succinate-induced current and clamp potential (Fig. 3*B*, ○). However, at each membrane potential, the observed current was considerably smaller for K114I than for WT.

We generated three additional mutants in which the lysine at position 114 was replaced by arginine, glutamic acid, and glutamine. The *I-V* relationships of K114E (Fig. 4*A*, ○), K114R (■), and K114Q (Fig. 4*B*, ○) are shown with those obtained in WT (Fig. 4, *A* and *B*, ●). K114R and K114Q showed potential-dependent, succinate-induced inward currents. The currents evoked by K114R were similar in magnitude to those induced by WT, whereas K114Q currents showed amplitudes much smaller than those of WT. The extrapolated reversal potential for these currents was approximately +70 mV, indicating that the currents were carried by sodium. The currents induced by K114E were small and reversed at −43.7 ± 4.3 mV.

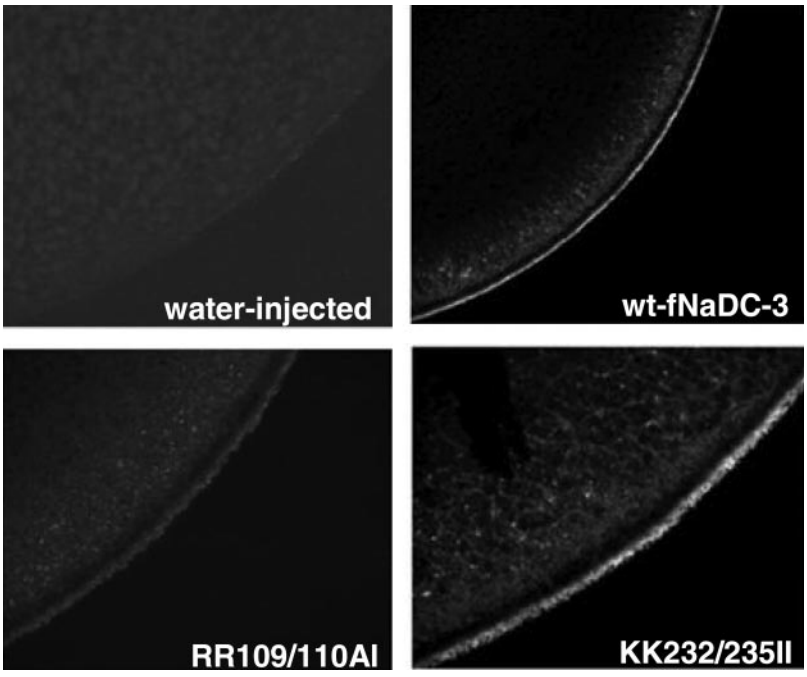

Fig. 2. Immunohistochemistry of wild-type (WT)-, RR109/110AI-, and KK232/235II-expressing oocytes. Devitellinized *Xenopus laevis* oocytes expressing WT-fNaDC-3 or its mutants were incubated with rabbit anti-NaDC-3 antibodies in a dilution of 1:50 followed by the secondary antibody Alexa Fluor 488 goat anti-rabbit in a dilution of 1:200. Sections (5 μm) were analyzed with a fluorescence microscope. *Top left*: water-injected oocyte. *Top right*: expression of WT-fNaDC-3. *Bottom left*: missing expression of mutant RR109/110AI. *Bottom right*: expression of mutant KK232/235II.

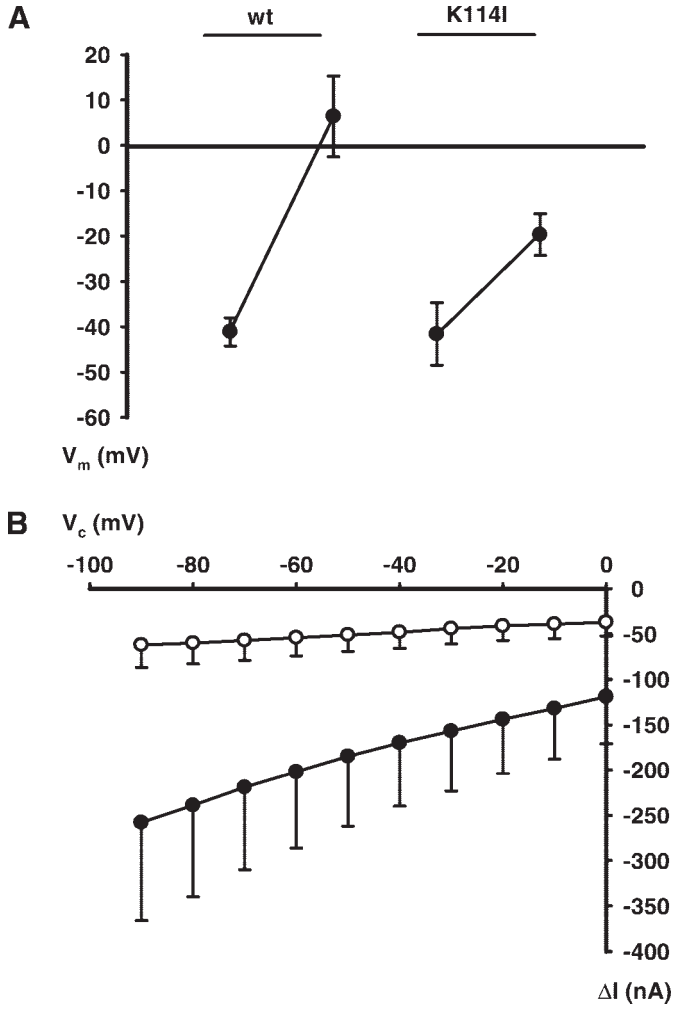

Fig. 3. Succinate-induced depolarization (*A*) and inward currents (*B*) in WT- and K114I-expressing oocytes. *A*: membrane potential (V_m) was measured under current-clamp conditions in the absence and presence of 1 mM succinate in control solution. Compared with WT, in K114I-expressing oocytes the succinate-induced depolarization was smaller. *B*: afterward, current-voltage relationships were obtained using the same oocytes. At all clamp potentials (V_c), the substrate-associated inward currents (ΔI) were smaller in K114I-expressing (○) than in WT-expressing oocytes (●). Data were obtained from 10 (WT) and 9 (K114I) oocytes from 4 donors.

To exclude the possibility that the decreased depolarization and currents were due to a lower degree of transporter expression, we first performed immunostaining. Figure 5 shows that all mutants, K114I, K114R, K114Q, and K114E, were present at the oocyte's membrane. Then, we performed [^{14}C]succinate uptake and current measurement simultaneously on the same oocytes. Each oocyte was clamped to −60 mV, and 68 μM succinate (18 μM [^{14}C]succinate plus 50 μM unlabeled succinate) was added to the perfusion chamber. Uptake and current were measured for 30 min under continuous voltage clamp. The experiment was repeated with different oocytes expressing either WT fNaDC3 or any of the mutants, or with water-injected "mock" oocytes. As shown in Fig. 6*A*, [^{14}C]succinate uptake was markedly higher in WT and all mutants compared with mock oocytes, indicating functional expression. Uptake by K114I and K114Q exceeded that of WT, whereas K114R and K114E showed [^{14}C]succinate uptake rates similar to WT. The succinate-induced inward current was much higher in WT-expressing oocytes than in mock cells (Fig. 6*B*). Mutant K114R showed an inward current of similar magnitude as WT. However, the mutants K114I, K114Q, and K114E exhibited significantly reduced inward currents, indicating a change in the electrogenicity of Na^+-succinate cotransport.

DISCUSSION

In renal proximal tubule cells, NaDC-3, the sodium-dependent dicarboxylate cotransporter, is located at the basolateral membrane. NaDC-3 carries a range of dicarboxylates, e.g., succinate, α-ketoglutarate, and protonated tricarboxylates such as divalent citrate (2). The identification of dicarboxylate and cation binding sites in NaDC-3 and the TM helixes involved in forming the translocation path remain areas of investigation. Because the cosubstrate (Na^+) and the substrates (di- and tricarboxylates) are charged, binding and translocation may involve charged amino acid residues within the NaDC-3 molecule, probably located near to or within the transmembrane helixes forming the as yet elusive transport pore.

As opposed to NaDC-3, considerable efforts have been undertaken to unravel amino acid residues involved in Na^+ and succinate binding of the rabbit NaDC-1. Mainly, amino acids in TMs 7, 8, 9, and 10 as well as the extracellular loop between

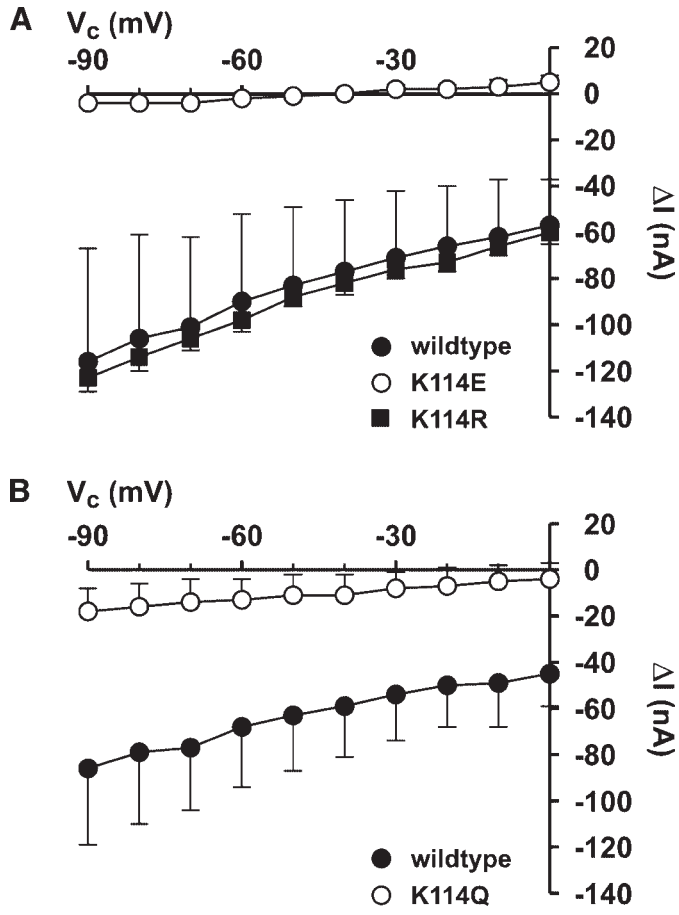

Fig. 4. Current-voltage relationships of WT, K114E, K114R, and K114Q. ΔI induced by 1 mM succinate was plotted as a function of V_c. *A*: currents evoked by K114E (○) and K114R (■) compared with WT currents (●). *B*: similar experiments performed with K114Q (○) and WT (●). Values are means ± SE of 7 oocytes from 3 donors.

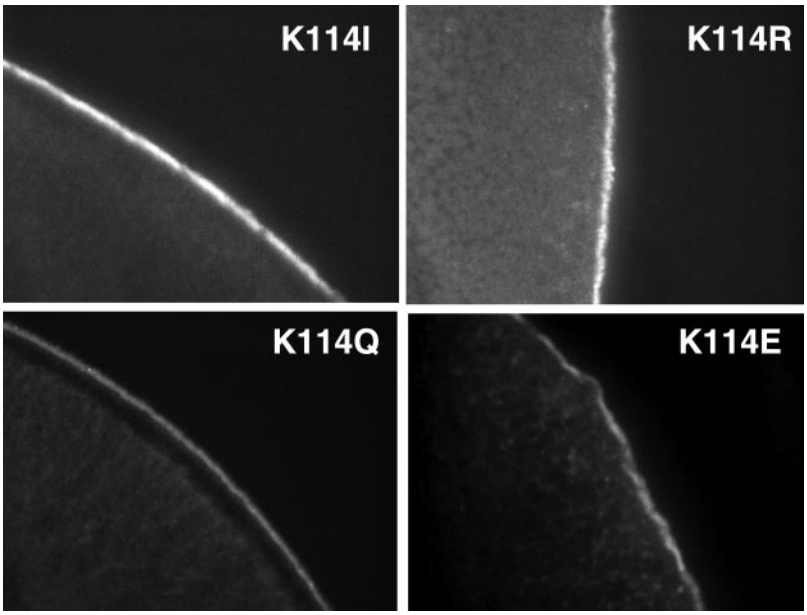

Fig. 5. Immunohistochemistry of mutant K114-expressing oocytes. Devitellinized *X. laevis* oocytes expressing K114I, K114R, K114Q, and K114E were incubated with rabbit anti-NaDC-3 antibodies in a dilution of 1:50 followed by the secondary antibody Alexa Fluor 488 goat anti-rabbit in a dilution of 1:200. Sections (5 μm) were analyzed with a fluorescence microscope.

TM 9 and 10 of rbNaDC-1 are accessible from the outside, interact with succinate, and/or are involved in Na^+-induced conformational changes (19). The affinity for succinate was altered when the residues K84 (intracellular loop between TM2 and 3 of rbNaDC-1), R349 (TM7), S372, D373 (TM8), and E475 (TM9) were mutated (7, 22, 36). Activation by Na^+ was changed, when residues S372 and D373 in TM8, and E475, A481, and T482 in TM9 were replaced by other amino acids (7, 18, 36). After being replaced with cysteine, most of the residues at positions 480–493 in the fifth extracellular loop (between TM9 and 10) were accessible for the water-soluble, membrane-impermeant SH reagent MTSET (18). Since Na^+ increased, and succinate decreased, accessibility, amino acids at the outer faces of TM9 and 10 and the connecting loop are involved in Na^+-induced binding of succinate.

In fNaDC-3, we mutated 4 arginines (R39, R109, R110, R503), 1 histidine (H14), and 10 lysines (K15, K36, K78, K114, K122, K232, K235, K374, K375, K548) within or near putative TM domains. Most mutants proved to be functional and exhibited Na^+-dependent [^{14}C]succinate uptake. Only the double mutants RR109/110AI and KK232/235II showed strongly reduced uptake rates. In TEVC experiments, all mutants except K114I and KK232/235II exhibited K_m values between 6 and 36 μM (WT: 22 μM) and maximal inward currents between −40 and −121 nA (WT: −55 nA).

The first conclusion to be drawn from these data is that the replacement of H14, K15, K36, R39, K78, K122, K374, K375, R503, and K548 by neutral amino acid residues appears to have no gross influence on the function of flounder renal NaDC-3. With regard to K36, R503, and K548, our results are in agreement with the mutational analysis of K34, A496, and R542 present at the respective positions in rbNaDC-1, which also did not show any changes in succinate transport (22, 23). The amino acids corresponding to R39, K78, K122, K374, and K375 have not been mutated in earlier studies on rbNaDC-1.

The replacements of the amino acid residues R109 and R110 in RR109/110AI, of K232 and K235 in KK232/235II, and of K114 by neutral and acidic amino acids did interfere with transport capacity or electrogenicity of the cotransporter. The replacement of RR109/110 in the second extracellular loop by alanine and isoleucine (RR109/110AI) led to a complete loss of function. Immunofluorescence studies revealed that the RR109/110AI protein was not expressed and did not appear at the plasma membrane of the oocytes. The arginines at positions 109 and 110 of NaDC-3 seem to be important, because they are conserved either as RR or as KR through all NaDC-1s, NaDC-3s, and NaCTs (alignment not shown). Mutational analysis of rbNaDC-1 demonstrated that the replacement of R108 (which corresponds to R110 in NaDC-3) by alanine reduced V_{max} without changing the affinity (22). The strong reduction of V_{max} suggested a low expression level of this mutant at the oocyte membrane. The studies on rbNaDC-1 and fNaDC-3 demonstrate the relevance of basic amino acids close to TM4 for proper expression and routing of the transporters to the plasma membrane.

The basic amino acids K232 and K235 are located within TM5. K235 is highly conserved through all NaDC-3s and NaCTs. NaDC-1s exhibit a glutamine at this position. The mutant KK232/235II showed a considerably reduced [^{14}C]succinate uptake and, in voltage-clamp experiments, barely detectable succinate-induced currents. Surprisingly, KK232/235II was present at the plasma membrane. K232 and K235 in TM 5 are, therefore, not involved in expression and targeting but may contribute to succinate binding and/or translocation.

Replacement of lysine 114 located in TM 4 by isoleucine was performed because K114 is highly conserved through all NaDC-3s (alignment not shown). In hNaDC-1, rbNaDC-1, and all NaCTs, an arginine is located at that position. [^{14}C]succinate uptake mediated by K114I was slightly higher than that of WT. In contrast, succinate-induced depolarization and currents were considerably smaller than those observed for WT. Even when tested simultaneously in the same oocytes, [^{14}C]succinate uptake was still higher for K114I, but the induced inward current was significantly smaller for K114I than for WT fNaDC-3, suggesting an altered electrogenicity.

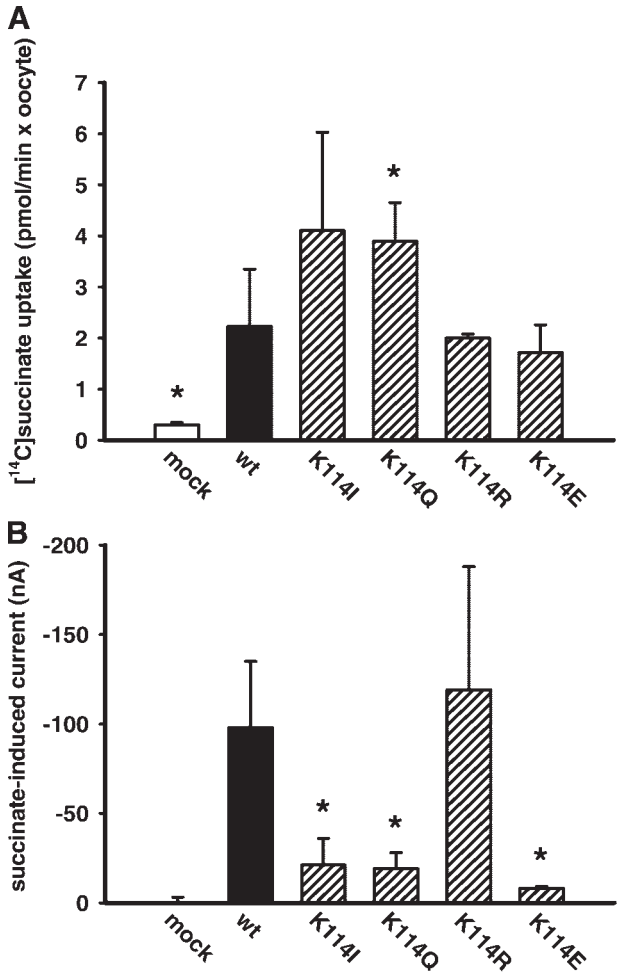

Fig. 6. Simultaneous measurement of succinate uptake and succinate-induced current of WT and K114 mutants. [^{14}C]succinate uptake and initial [^{14}C]succinate-induced current were measured simultaneously at 68 μM succinate (18.1 μM [^{14}C]succinate plus 50 μM unlabeled succinate) in the same oocyte clamped at −60 mV. After a 30-min recording of the [^{14}C]succinate-induced current, oocytes were washed 3 times with ice-cold control solution and lysed by 1 M NaOH for liquid scintillation counting. *A*: succinate uptake of WT and K114 mutants is expressed in pmol·min^{-1}·oocyte^{-1}. *B*: currents induced by 68.1 μM [^{14}C]succinate (in nA). Simultaneous measurements were performed in 3–9 oocytes from 2–7 donors. *$P < 0.01$ vs. WT fNaDC-3.

For further characterization, we substituted lysine 114 with the basic amino acid arginine, the acidic amino acid glutamic acid, and the neutral amino acid glutamine. Mutant K114R revealed the same functional characteristics as WT with respect to succinate uptake and succinate-induced current. Substitution of lysine by glutamine (K114Q) or glutamic acid (K114E) led to a [^{14}C]succinate uptake not different from WT, and a decrease in succinate-induced inward currents as was found for K114I. From these experiments it can be inferred that a positive charge must be present at position 114 for fully electrogenic sodium-succinate cotransport.

A possible reason for decreased succinate-induced currents at unaltered [^{14}C]succinate uptake may be a change in the sodium:succinate stoichiometry. Whereas WT translocates three sodium ions with each succinate molecule, K144I may vary between a 2:1 and a 3:1 stoichiometry, leading to a decreased inward current and a decreased membrane depolarization. Alternatively, electroneutrality in the K114I mutant may result from a backflux of a cation (Na^+, K^+, H^+) during each transport cycle, or a symport of sodium, succinate, and a monovalent anion (Cl^-, OH^-). Clearly, more experiments are needed to define the exact transport mode of mutant K114I and to find out the Na^+ binding sites in NaDC-3.

Usually, negatively charged amino acid residues are important for recognition, selectivity, and binding of cations. D804 and D808 residues in the α-subunit of the Na^+-K^+-ATPase are essential for the interaction with Na^+ and K^+ ions (25). The transport of Na^+ and K^+ mediated by the glutamate transporter GLT1 depended on amino acid residues Y403 and E404 (26, 38). In rabbit NaDC-1, D373 in TM8 and E475 in TM9 have been found to be critically involved in interaction with Na^+ and succinate (23). That the replacement of a positive charge at position 114 interferes with the binding of one of the three sodium binding sites is not easy to reconcile with these findings. In NaDC-3, however, K114 may be needed to properly position other helixes involved in binding of Na^+.

In conclusion, the mutational analysis of basic amino acid residues in fNaDC-3 documented the importance of the conserved R109 and R110 for the expression at the plasma membrane. K232 and K235 near TM5 are probably involved in substrate recognition and/or transport. K114 located in TM4 is essential for fully electrogenic Na^+-succinate cotransport.

ACKNOWLEDGMENTS

The authors thank S. Holpert and I. Markmann for technical assistance.

GRANTS

This work was supported by the DFG grants BU571/7–5, BU998/2–3, and STE435/2–4.

REFERENCES

1. **Bakhiya N, Bahn A, Burckhardt G, and Wolff N.** Human organic anion transporter 3 (hOAT3) can operate as an exchanger and mediate secretory urate flux. *Cell Physiol Biochem* 13: 249–256, 2003.
2. **Burckhardt BC and Burckhardt G.** Transport of organic anions across the basolateral membrane of proximal tubule cells. *Rev Physiol Biochem Pharmacol* 146: 95–158, 2003.
3. **Burckhardt BC, Steffgen J, Langheit D, Muller GA, and Burckhardt G.** Potential-dependent steady-state kinetics of a dicarboxylate transporter cloned from winter flounder kidney. *Pflügers Arch* 441: 323–330, 2000.
4. **Chen X, Tsukaguchi H, Chen XZ, Berger UV, and Hediger MA.** Molecular and functional analysis of SDCT2, a novel rat sodium-dependent dicarboxylate transporter. *J Clin Invest* 103: 1159–1168, 1999.
5. **Chen XZ, Shayakul C, Berger UV, Tian W, and Hediger MA.** Characterization of a rat Na^+-dicarboxylate cotransporter. *J Biol Chem* 273: 20972–20981, 1998.
6. **George RL, Huang W, Naggar HA, Smith SB, and Ganapathy V.** Transport of N-acetylaspartate via murine sodium/dicarboxylate cotransporter NaDC3 and expression of this transporter and aspartoacylase II in ocular tissues in mouse. *Biochim Biophys Acta* 1690: 63–69, 2004.
7. **Griffith DA and Pajor AM.** Acidic residues involved in cation and substrate interactions in the Na^+/dicarboxylate cotransporter, NaDC-1. *Biochemistry* 38: 7524–7531, 1999.
8. **Hagos Y, Burckhardt BC, Larsen A, Mathys C, Gronow T, Bahn A, Wolff NA, Burckhardt G, and Steffgen J.** Regulation of sodium-dicarboxylate cotransporter-3 from winter flounder kidney by protein kinase C. *Am J Physiol Renal Physiol* 286: F86–F93, 2004.
9. **Hentschel H, Burckhardt BC, Scholermann B, Kuhne L, Burckhardt G, and Steffgen J.** Basolateral localization of flounder Na^+-dicarboxylate cotransporter (fNaDC-3) in the kidney of *Pleuronectes americanus*. *Pflügers Arch* 446: 578–584, 2003.
10. **Huang W, Wang H, Kekuda R, Fei YJ, Friedrich A, Wang J, Conway SJ, Cameron RS, Leibach FH, and Ganapathy V.** Transport of N-acetylaspartate by the Na^+-dependent high-affinity dicarboxylate trans-

porter NaDC3 and its relevance to the expression of the transporter in the brain. *J Pharmacol Exp Ther* 295: 392–403, 2000.
11. **Inoue K, Fei YJ, Huang W, Zhuang L, Chen Z, and Ganapathy V.** Functional identity of *Drosophila melanogaster* Indy as a cation-independent, electroneutral transporter for tricarboxylic acid-cycle intermediates. *Biochem J* 367: 313–319, 2002.
12. **Inoue K, Zhuang L, Maddox DM, Smith SB, and Ganapathy V.** Structure, function, and expression pattern of a novel sodium-coupled citrate transporter (NaCT) cloned from mammalian brain. *J Biol Chem* 277: 39469–39476, 2002.
13. **Kekuda R, Wang H, Huang W, Pajor AM, Leibach FH, Devoe LD, Prasad PD, and Ganapathy V.** Primary structure and functional characteristics of a mammalian sodium-coupled high affinity dicarboxylate transporter. *J Biol Chem* 274: 3422–3429, 1999.
14. **Knauf F, Rogina B, Jiang Z, Aronson PS, and Helfand SL.** Functional characterization and immunolocalization of the transporter encoded by the life-extending gene Indy. *Proc Natl Acad Sci* 99: 14315–14319, 2002.
15. **Markovich D and Murer H.** The SLC13 gene family of sodium sulphate/carboxylate cotransporters. *Pflügers Arch* 447: 594–602, 2003.
16. **Oshiro N, King SC, and Pajor AM.** Transmembrane helices 3 and 4 are involved in substrate recognition by the Na^+-dicarboxylate cotransporter, NaDC1. *Biochemistry* 45: 2302–2310, 2006.
17. **Pajor AM.** Molecular properties of sodium/dicarboxylate cotransporters. *J Membr Biol* 175: 1–8, 2000.
18. **Pajor AM.** Conformationally sensitive residues in transmembrane domain 9 of the Na^+-dicarboxylate co-transporter. *J Biol Chem* 276: 29961–29968, 2001.
19. **Pajor AM.** Molecular properties of the SLC13 family of dicarboxylate and sulfate transporters. *Pflügers Arch* 451: 597–605, 2006.
20. **Pajor AM, Gangula R, and Yao X.** Cloning and functional characterization of a high-affinity Na^+-dicarboxylate cotransporter from mouse brain. *Am J Physiol Cell Physiol* 280: C1215–C1223, 2001.
21. **Pajor AM, Hirayama BA, and Loo DD.** Sodium and lithium interactions with the Na^+-dicarboxylate cotransporter. *J Biol Chem* 273: 18923–18929, 1998.
22. **Pajor AM, Kahn ES, and Gangula R.** Role of cationic amino acids in the Na^+-dicarboxylate co-transporter NaDC-1. *Biochem J* 350: 677–683, 2000.
23. **Pajor AM and Randolph KM.** Conformationally sensitive residues in extracellular loop 5 of the Na^+-dicarboxylate cotransporter. *J Biol Chem* 280: 18728–18735, 2000.
24. **Pajor AM and Valmonte HG.** Expression of the renal Na^+-dicarboxylate cotransporter, NaDC-1, in COS- 7 cells. *Pflügers Arch* 431: 645–651, 1996.
25. **Pedersen PA, Rasmussen JH, Nielsen JM, and Jørgensen PL.** Identification of Asp804 and Asp808 as Na^+ and K^+ coordinating residues in alpha-subunit of renal Na,K-ATPase. *FEBS Lett* 400: 206–210, 1997.
26. **Pines G, Zhang Y, and Kanner BI.** Glutamate 404 is involved in the substrate discrimination of GLT-1, a (Na^+ + K^+)-coupled glutamate transporter from rat brain. *J Biol Chem* 270: 17093–17097, 1995.
27. **Rogina B, Reenan RA, Nilsen SP, and Helfand SL.** Extended life-span conferred by cotransporter gene mutations in *Drosophila*. *Science* 290: 2137–2140, 2000.
28. **Sekine T, Cha SH, Hosoyamada M, Kanai Y, Watanabe N, Furuta Y, Fukuda K, Igarashi T, and Endou H.** Cloning, functional characterization, and localization of a rat renal Na^+-dicarboxylate transporter. *Am J Physiol Renal Physiol* 275: F298–F305, 1998.
29. **Sekine T, Watanabe N, Hosoyamada M, Kanai Y, and Endou H.** Expression cloning and characterization of a novel multispecific organic anion transporter. *J Biol Chem* 272: 18526–18529, 1997.
30. **Steffgen J, Burckhardt BC, Langenberg C, Kühne L, Müller GA, Burckhardt G, and Wolff NA.** Expression cloning and characterization of a novel sodium-dicarboxylate cotransporter from winter flounder kidney. *J Biol Chem* 274: 20191–20196, 1999.
31. **Sweet DH, Chan LM, Walden R, Yang XP, Miller DS, and Pritchard JB.** Organic anion transporter 3 (*Slc22a8*) is a dicarboxylate exchanger indirectly coupled to the Na^+ gradient. *Am J Physiol Renal Physiol* 284: F763–F769, 2003.
32. **Wang H, Fei YJ, Kekuda R, Yang-Feng TL, Devoe LD, Leibach FH, Prasad PD, and Ganapathy V.** Structure, function, and genomic organization of human Na^+-dependent high-affinity dicarboxylate transporter. *Am J Physiol Cell Physiol* 278: C1019–C1030, 2000.
33. **Wang J, Chen X, Zhu H, Peng L, and Hong Q.** Relationship between aging and renal high-affinity sodium-dependent dicarboxylate cotransporter-3 expression characterized with antifusion protein antibody. *J Gerontol A Biol Sci Med Sci* 58: B879-B888, 2003.
34. **Wirthensohn G and Guder WG.** Renal substrate metabolism. *Physiol Rev* 66: 469–497, 1986.
35. **Wolff NA, Werner A, Burkhardt S, and Burckhardt G.** Expression cloning and characterization of a renal organic anion transporter from winter flounder. *FEBS Lett* 417: 287–291, 1997.
36. **Yao X and Pajor AM.** Arginine-349 and aspartate-373 of the Na^+-dicarboxylate cotransporter are conformationally sensitive residues. *Biochemistry* 41: 1083–1090, 2002.
37. **Zhang FF and Pajor AM.** Topology of the Na^+-dicarboxylate cotransporter: the N-terminus and hydrophilic loop 4 are located intracellularly. *Biochim Biophys Acta* 1511: 80–89, 2001.
38. **Zhang Y, Bendahan A, Zarbiv R, Kavanaugh MP, and Kanner BI.** Molecular determinant of ion selectivity of a (Na^+ + K^+)-coupled rat brain glutamate transporter. *Proc Natl Acad Sci USA* 95: 751–755, 1998.